Chapter

Eruption Types and Processes in the Guamsan Caldera, Korea

Sang Koo Hwang

Abstract

The Guamsan caldera is associated with the Guamsan Tuff and rhyolitic intrusions. The Guamsan Tuff consists of dominant ash-flow tuffs with some volcanic breccias and fallout tuffs. The breccias comprise block and ash-flow breccia near a vent and caldera-collapse breccia near a ring fracture. The lower member of the ash-flow tuffs is produced from pyroclastic flow-forming eruptions with any ash-cloud falls on the flow units, whereas the upper member is formed by many ash-flow from boiling-over eruptions. The rhyolitic intrusions are divided into intracaldera plug and ring dikes. The volcanic activities in the caldera exhibit the volcanic processes along a caldera cycle together with eruption types during 63.77–60.1 Ma. The activities began with pelean eruption that occurred with block and ash-flows from lava dome collapse, progressed through expanded pyroclastic flows and ash-cloud falls by pyroclastic flow-forming eruptions from a single central vent, and transmitted with non-expanded ash-flows from boiling-over eruptions along multiple ring fissure vents. Then the caldera collapse induced any translations into multiple ring fissure vents from an earlier single central vent. The boiling-over eruptions were followed by effusive eruptions along which rhyolitic magma was injected as a small plug and ring dikes with some lava domes on the surface.

Keywords: Guamsan caldera, Guamsan tuff, ring dikes, pyroclastic flow-forming eruptions, boiling-over eruptions, effusive eruptions

1. Introduction

Juwangsan volcanic field, located in the northeastern part of Gyeongsang basin, comprises several calderas associated with the succession of ash-flow tuff—caldera—ring dike. The evolution of Guamsan caldera, in the central part of the volcanic field, has been reported on in detail by a previous study [1, 2]. However, the eruption types in the caldera were not investigated. This study thus intends to interpret eruptive types and volcanic processes of the volcanic rocks associated with the caldera.

The strata in the Gyeongsang basin are so deeply eroded that the volcanic rocks are dominantly left inside the calderas. Likewise, the Guamsan caldera area has been so significantly eroded and so deep in valleys that it provides us with an excellent laboratory field that not only reveals almost all of the volcanic rocks related to the caldera but also reveals the intrusions corresponding to volcanic roots. Thereby, the Guamsan caldera area exposes the Guamsan Tuff as well as diverse intracaldera

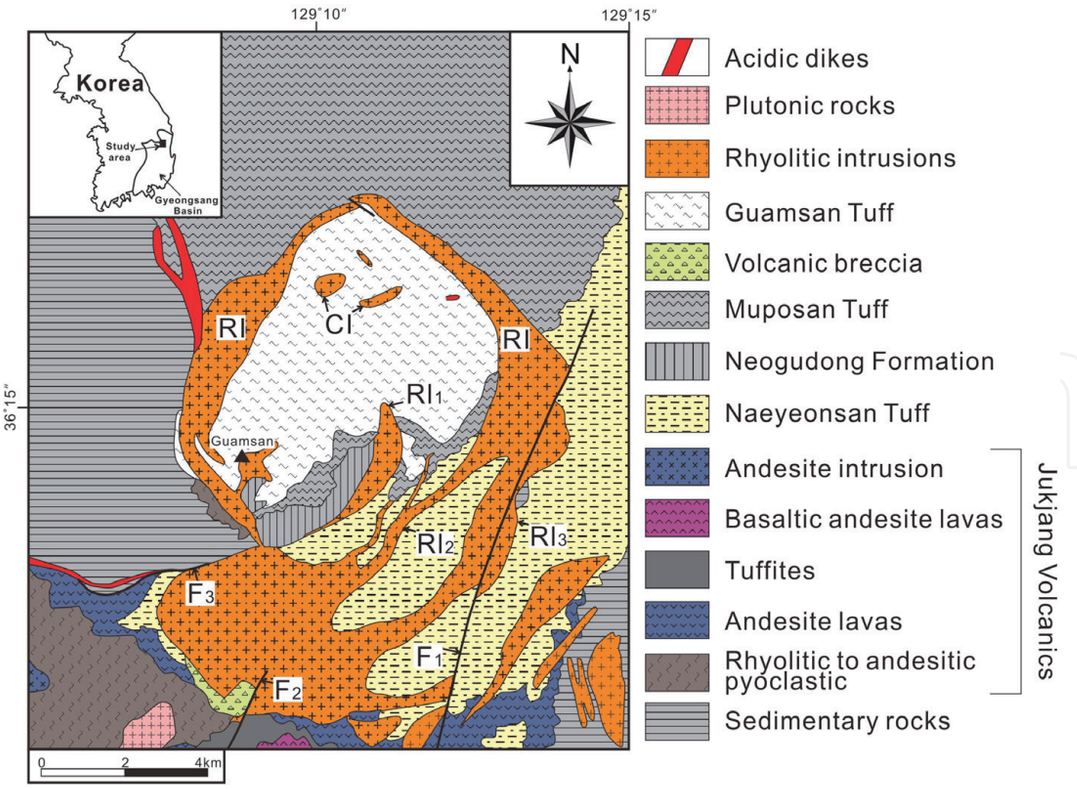

Figure 1.
Generalized geological map in and around the Guamsan caldera in the northeastern Gyeongsang basin. RI, ring intrusions (RI, inner ring dike; RI_2, intermediate ring dike; RI_3, outer ring dike); CI, intracaldera intrusions; F1, Sampo fault; F2, Jayangcheon fault; EW, trending fault.

intrusions and ring dikes (**Figure 1**). The lithofacies and sequences of these extrusive rocks and intrusive rocks are sufficient to interpret eruption types and reconstruct volcanic processes in the Guamsan caldera.

Eruption types and volcanic processes before and after caldera collapse will be discussed in this study. The ultimate results reveal that the volcanic activities in Gyeongsang Basin are not only related with caldera volcanisms but are also significant for understanding the characteristics of the igneous processes. Further, the consequences will contribute to the understanding of other volcanisms and processes in the calderas as well as their comparative effects.

2. Geological setting

The Gyeongsang basin has a broad distribution of volcanic rocks which are products of the Late Cretaceous to Early Paleogene calc-alkalic volcanism in the subduction zone along the Eurasian continental margin [3–6]. These volcanic rocks are mostly distributed in the Yucheon subbasin and are also found in the region between southeastern Yeongyang subbasin and mid-eastern Euiseong subbasin; this region belongs to the Juwangsan volcanic field.

The volcanic rocks occurring in the field mostly consist of extrusive rocks accompanied by small amounts of intrusive rocks. The extrusive rocks are placed on sedimentary rocks of the Hayang Group and can be roughly categorized into lower basic to intermediate volcanic rocks and upper acidic volcanic rocks. The former extrusive rocks comprise the stratigraphic units of Daejeonsa Basalt, Ipbong Andesite, and Jukjang Volcanics. The latter extrusive rocks consist of Jipum Volcanics (68.5 Ma in [7]), Juwangsan Tuff, Naeyeonsan Tuff, Neogudong Formation, Muposan Tuff (67.08 Ma in [8]), and Guamsan Tuff (63.77 ~ 60.1 Ma in [9]).

The intrusive rocks comprise rhyolitic intrusions relevant to the caldera as well as biotitic granite and felsite dikes irrelevant to the caldera. The rhyolitic intrusions correspond to the volcanic rocks of postcaldera, which can be divided into intracaldera intrusions and ring dikes. The biotitic granite is exposed as small stocks, whereas the felsite is exposed as linear dikes.

In the area, the geology is cut by the Sampo fault and Jayangcheon fault, the strike-slip fault running southwest from northeast and is depressed by a fault running west from east (**Figure 1**).

3. Guamsan caldera

The Guamsan caldera is bound along the structural line as determined by the outer ring dike. The caldera is approximately 9.2 km in maximum diameter and 8.0 km in minimum diameter [1]; the resulting internal area is then approximately 66.0 km in [2].

The intracaldera Guamsan Tuff has a contact with the underlying Muposan Tuff, with the ring dike intervening between two units, suggesting that the former unit has been subsided as compared to the latter unit. This can be counted as direct evidence of the subsidence by the collapse of a caldera. The welding foliation and bedding in the volcanic and sedimentary rocks generally represent a basin structure like a bowl shape, which has steep to gentle dips inwardly from the caldera margin. The structure suggests a direct subsidence from the collapse of the caldera. The caldera block shows an asymmetrical feature that was collapsed to 900 m along the northern margin, whereas it was collapsed to 300 m along the southern margin [1].

Therefore, the caldera was formed by down-sagging and ring-faulting. Based on comprehensive integration of these evidences, the caldera is classified as one of the asymmetrical cylindrical caldera [1].

4. Guamsan Tuff

Guamsan Tuff refers to a stratigraphic unit composed of volcanic breccias, ash-flow tuffs, fallout tuffs, and tuffites derived from the Guamsan caldera (**Figure 2**). The stratigraphic unit mostly consists of ash-flow tuffs that are only distributed inside the caldera (**Figure 1**). Though it was thick tuffs accumulated from the radial spreading of voluminous ash flow erupted from the crater hidden inside the caldera, it now remains only inside the caldera, due to prolonged erosion and denudation. The remaining body exposes its cross sections of the lower member (63.77 Ma in [9]) to upper member (60.1 Ma in [9]), because it has not only deep valleys that have been made by erosion but is also inclined northward by an igneous intrusion in the southern outer part of the caldera. The tuffs range 72~78% SiO_2 in composition, which indicates high silica to low silica [2].

The author describes lithofacies and mutual relations in the Guamsan Tuff and reconstructs the evolution processes of complex volcanic events from the volcanic ejecta.

4.1 Volcanic breccias

Volcanic breccias can be subdivided into two lithofacies of disorganized massive breccia and chaotic massive breccia.

The disorganized massive breccia mostly consists of monolithic blocks of rhyolite and accompanies rare accessory blocks of andesite and welded tuff.

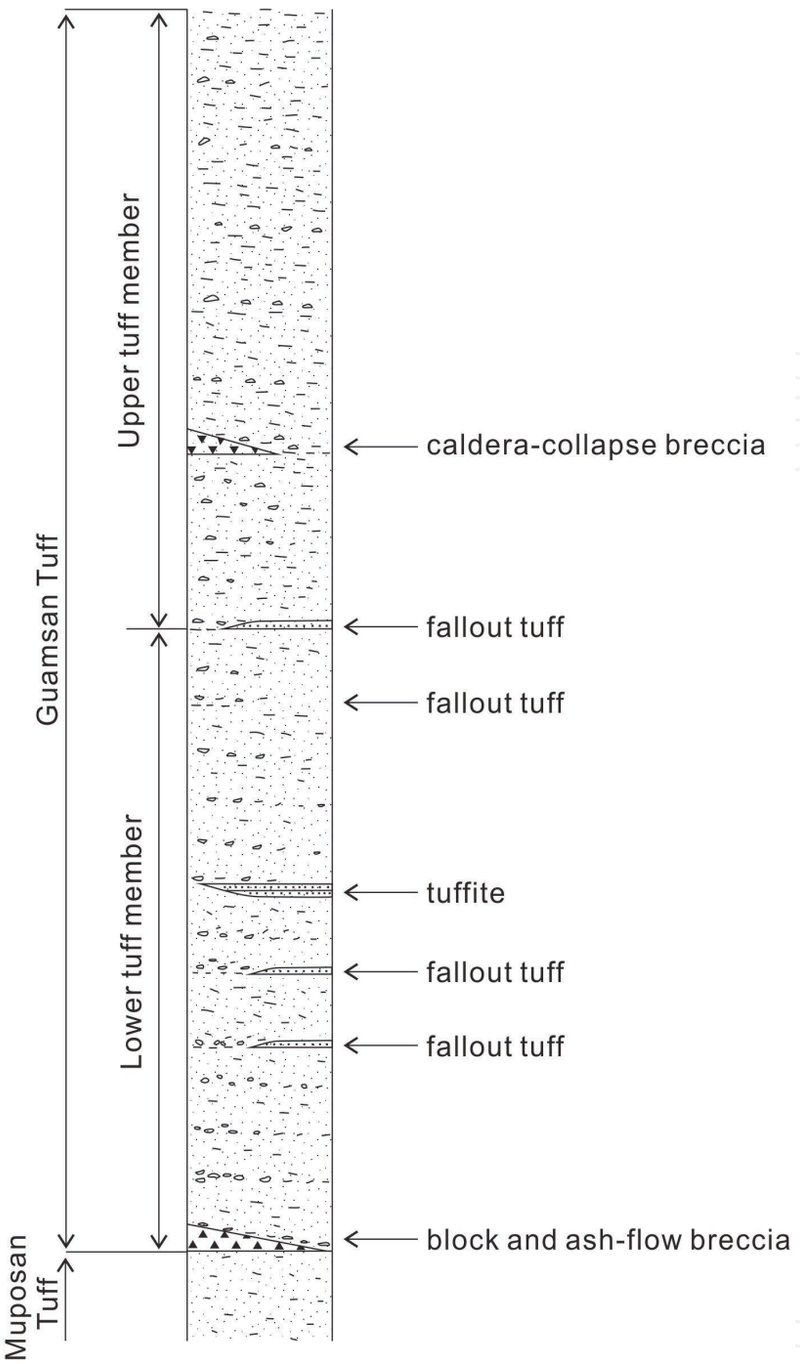

Figure 2.
Typical columnar section of the Guamsan tuff, which exhibits variations in stratigraphic units that comprise volcanic breccias, fallout tuffs, and tuffites in entire ash-flow tuffs.

The blocks are typically 5~15 cm in diameter, rarely reaching over 1 m, and are subround to subangular in shape (**Figure 3a**). The matrix consists of pale gray to gray ash that supports the blocks. The lithofacies exhibit the vertically thick lenticular form with laterally poor continuity. Typically, the lithofacies may be very thick in topographic depression and very thin on topographic high. Except for the blocks, it resembles lapilli tuff without internal stratification and grading. The lithofacies occur as basal breccia in the southwestern side of the outer ring dike (**Figure 4a**), from which the breccia gradually becomes grading into lapilli tuff in going northeastward. Along the emplaced site, it suggests that the breccia could be significantly different in terms of the mechanism forming the lithofacies. This can be supported by the fact that the trend is significantly different from those of other rock units in granulometric classification diagram.

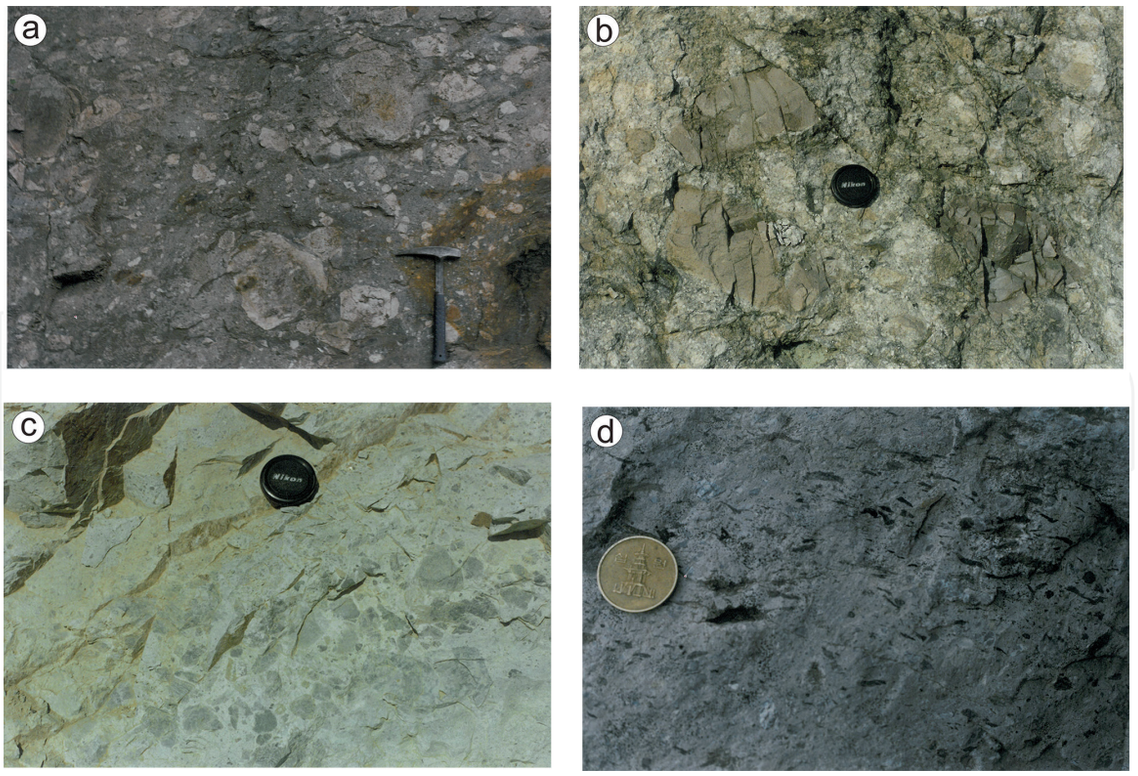

Figure 3.
Photographs in the Guamsan tuff. (a) Disorganized massive breccia in a near-vent facies; (b) chaotic massive breccia near the northern caldera margin; (c) graded lapilli tuff; (d) eutaxitic fabric in the middle part of the thick tuff and lapilli tuff bed.

The breccia embraces the southwestern side of the ring dike (**Figure 1**) and overlies the Naeyeonsan Tuff, cutting the Jugjang Volcanics. The lithofacies are correlated to the lowermost part of the Guamsan Tuff, based on sulfide alteration, stratigraphic relation, and lithologic correlation [1]. Therefore, the breccia may be considered as pyroclastic rocks accumulated from pyroclastic flows on a cone slope. The mechanism forming the pyroclastic flow may be dominated by the collapse of lava dome, because of the rhyolitic monolithic blocks. Namely, the pyroclastic flow-forming eruption type may be of the block and ash-flow phase that flowed along the slope from the collapse of active lava dome. Here, such lithofacies may indicate that it would be a near-vent facies, suggesting the initiation of volcanism in the Guamsan area.

Chaotic massive breccia, while it cannot be expressed on a geological map, is intercalated as a wedge shape between ash-flow tuffs in the lower part of the upper tuff member. The lithofacies consist of many blocks of rhyolite and welded tuff, which range 10~20 cm in diameter and occasionally over 1 m (**Figure 3b**). Based on granulometry, the rock is classified as tuff breccia, of which the trend is very different from those of other rock units. The boundary surface of the lithofacies can be investigated due to the fact that it is deeply eroded enough to expose the base. Though the base is irregular, the flat top is discontinuing laterally to be connected to normal lapilli tuffs. The lithofacies have very irregularly chaotic internal structures, which are cut by small faults (**Figure 3b**). The lithofacies, which occur sporadically in a valley adjacent to the northern ring fracture zone, are intercalated stratigraphically in the middle part of the Guamsan Tuff (**Figure 4b**). These facts suggest that the lithofacies had been produced by gravitational sliding of blocks or debris flow from caldera wall along the ring fracture zone. Therefore, many blocks around 1 m in diameter are observed around the collapse zone. Therefore, the breccia is considered as a caldera-collapse breccia, which is classified as the debris-flow phase by the caldera collapse. In addition, the lithofacies are thought to suggest a vent transition that indicates fissure eruption. If the eruption

was initiated along the fissure, then it may have left many lithic fragments from the erosion of the vent walls. However, the content of lithic fragment decreases rapidly as it goes upward; this is a result of widening the conduit without erosion along caldera collapse due to the outward dipping of the fracture zone [1].

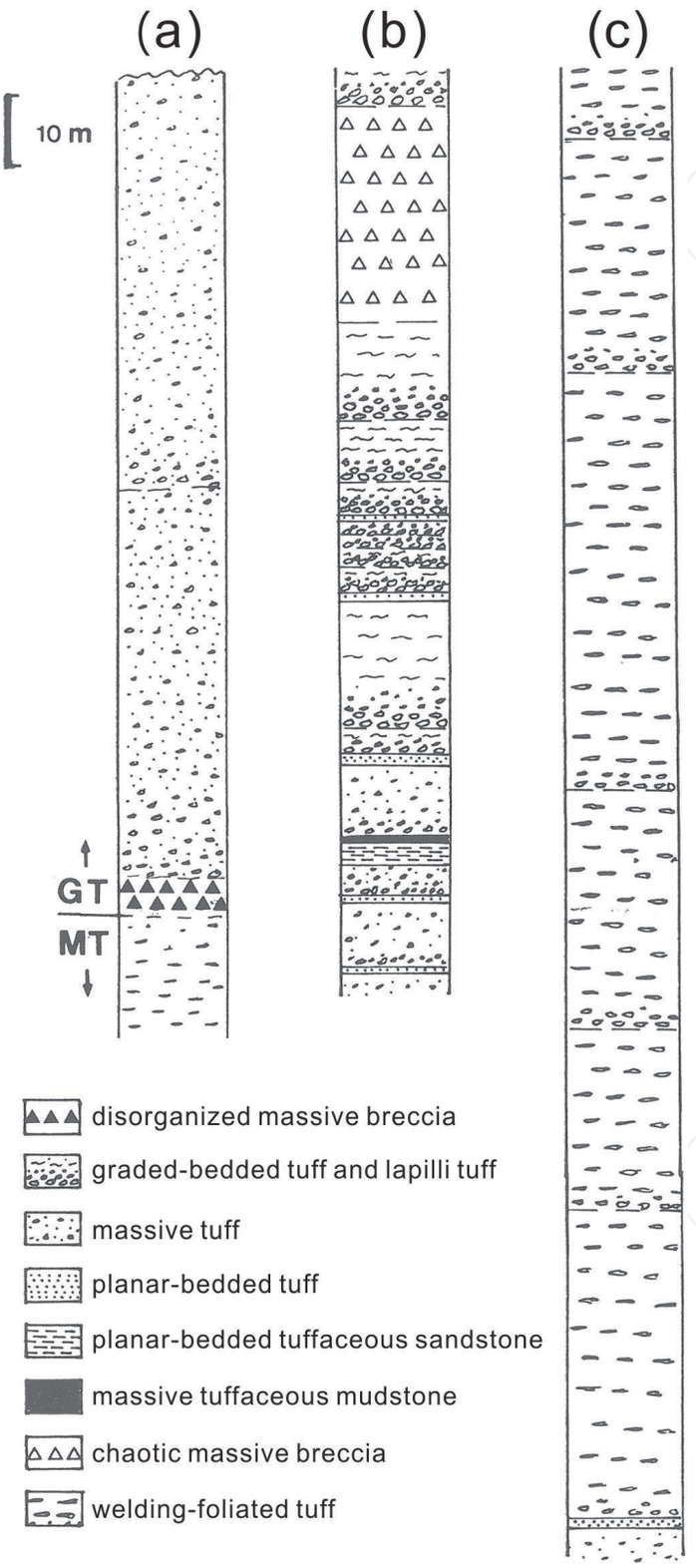

Figure 4.
Stratigraphic sections displaying variations in lithofacies of the Guamsan tuff (GT), underlain by the Muposan tuff (MT). (a) Lower member in the proximal zone; (b) lower member in the distal zone; (c) upper member of the Guamsan tuff.

4.2 Ash-flow tuffs

Lithofacies in the ash-flow tuffs comprises the graded tuff and lapilli tuff bed, massive tuff bed, and welding-foliated tuff bed.

The graded tuff and lapilli tuff beds exhibit whitish gray to pale gray color and are classified as lithic-rich vitric tuff consisting of lithics and pumice lapilli in the volcanic ash matrix. On the whole, the lithic lapilli are rich in the lower part, whereas pumice lapilli are more or less rich in the upper part. Therefore, lithics show a normal grading that gradually decrease upward in grain size within a single bed (**Figure 3c**). The matrix is composed of coarse ash, which is relatively richer than lapilli in the upper part. The lithofacies range from 2 to 20 cm in thickness and show laterally well extensibility. They represent eutaxitic fabric due to slightly welding in a thick single bed (**Figure 3d**), with lithics accumulated in its base (**Figure 5a**). The rock facies dominantly appear in the lower tuff member, whereas they occur in the lower part of the upper tuff member (**Figure 4a, b**). The grading in the lithofacies suggests a column collapse phase that was derived from the collapse of the high eruption column produced by a huge explosion. Then, collapsed tephra creates strongly fluidized pyroclastic flow that is supported by rising fluids in the same way as water vapor, etc., and dense lithics in flowing result in gradual sorting by the difference in final falling velocities.

Massive tuff bed is a lithic-rich vitric tuff that consists of lithics with various colors and a small amount of pumices. The matrix usually exhibits a whitish gray, pale gray, or pale bluish green color, whereas the lithics exhibit a dark gray, pale brown, or dark bluish green color; the pumices are mostly tinged with whitish gray color (**Figure 5b**). The matrix shows a massive appearance because it has very

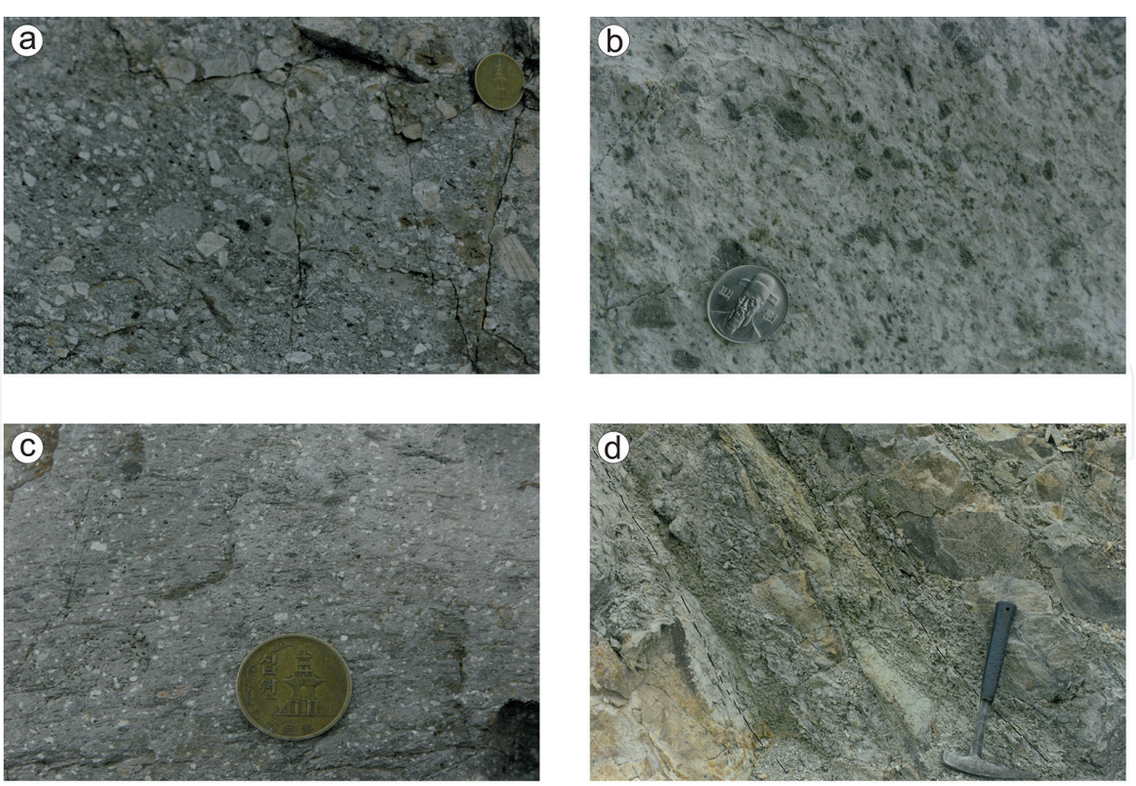

Figure 5.
Photographs in the Guamsan tuff. (a) Lithic-rich zone in the lower part of the thick tuff and lapilli tuff bed; (b) pale gray massive tuff; (c) dark gray welding-foliated tuff in the upper member; (d) planar-bedded tuff beds intercalated between ash-flow tuff beds in the lower member.

abundant content and very poor sorting. The lithics exhibit very weak grading, with them accumulated at the base. The thickness ranges from 4 to 25 m in the bed, the boundary of which is distinguished by the accumulation of lithics in a single bed. The lithofacies mostly occur in the lower tuff member (**Figure 4a**) and are mostly plotted into the tuff field. Under a microscope, the tuff has a small amount of plagioclase and orthoclase phenocrysts, as well as extremely rare biotite and opaque minerals. Vitric shards appear intact as skeletal, crescent, and "Y" shapes in the lower part; their outlines sometimes appear by devitrification. Accordingly, they exhibit almost a vitroclastic fabric due to non-welding to partial welding in the lowermost part. However, the lower tuff member produces weak welding foliations by the gradual flattening of pumices and shards with an increase in welding degree, when going up the member. According to the poor sorting, massive bedding, very thick beds, and non-welding, it suggests that the lithofacies were emplaced as ash flows of tephra accumulated from the collapse of relatively high eruption column created by a little huge explosion. The weak grading of lithics signifies the weak fluidization of the ash flow. The abundance in matrix also suggests reduced escapement of volcanic ash from the ash flow due to weak fluidization. Therefore, the lithofacies indicate that they were emplaced by slightly fluidized ash flow from collapse of the high eruption column. However, the increase in welding degree going upward indicates a gradual decrease in the height of the eruption column as well as a gradual increase in the discharge volume.

The welding-foliated tuff bed occurs only in the upper tuff member (**Figure 4c**). The matrix, gray to dark gray in color, corresponds to a vitric tuff that includes a few of plagioclase without quartz grain. Although the tuff on the whole is not sorted and has no stratifications, it is welded so seriously that it shows welding foliation similar to lava together with any features representing high fluidity during its emplacement. Additionally, although the boundary of each flow unit could be determined because of the abundance in lithics at the base, the other boundaries may not be observed as they recede from almost complete welding. Commonly, despite the fact that the ash-flow tuff bed ideally has a surge tuff bed at the base (layer 1) and a fallout tuff bed on the top (layer 3), they are not discovered (**Figure 4c**).

The lithofacies include rare lithics, which are mostly lapilli 2~5 cm in size. Vitric ash and pumices are densely welded and have welding foliations (**Figure 5c**). Pumices exhibit a dark gray color and are extremely flattened by the thick superposition of many ash flows, but they are still difficult to detect due to their small size. They are not easily recognizable as they exhibit aspects similar to lava on fresh surfaces. However, because lithics in the lithofacies are, although small in size, concentrated on the base of flow units, they are used to distinguish the single flow units. Under a microscope, the lithofacies occur as a small amount of plagioclase and alkali feldspars as microphenocrysts and rarely quartz, biotite, and opaque minerals. The pumices are devitrified to be crystalized as micrographic fabrics of silica and feldspars or as mosaic fabrics by vapor-phase crystallization in the core. Therefore, although the lithofacies exhibit welded foliation by dense welding of pumices and shards, they show eutaxitic fabric in the lower part and parataxitic fabric in the middle part; they then transform into the vitrophyric fabric in the upper part, of which is difficult to recognize pyroclastic structure. That is, the tuff represents the vitrophyric fabric similar to obsidian showing no traces of devitrification in spite of the gradual increase in welding degree going upward.

The poor sorting and welding foliation indicate that the lithofacies were emplaced from ash flows. No occurrence of ash cloud-derived fallout tuff in any of the sections may reflect its location proximal to the eruption center or short emplacement time between flow units due to successive eruptions. The abundance in lithics in the base suggests that the lithics were lagged downward by the lateral

movement of ash flows, even during a short time [10]. The sufficiently dense welding to have an indistinct boundary between fiammes and matrix suggests that they were significantly liquefied by almost complete welding under high temperatures. Based on the dense welding, as well as the sparsity or smaller size of phenocrysts in the upper part of the ash-flow tuff, the lithofacies indicate that they were emplaced by ash flows of relatively high temperature. Regarding the severe devitrification, the lithofacies indicate that the cooling period was relatively long by maintaining a longer time under high temperature by the reduction of heat loss, because of thick accumulation by rapid ash flows from the collapse of low eruption column.

The textural homogeneity, greater thickness, and denser welding reflect the sedimentary facies created by less fluidized non-expanded ash flows that have slow speed and less loss of volcanic ash into ash cloud, because they were originally erupted from hotter magma [11]. Such ash-flow phases also suggest that they originated from nonviolent voluminous eruptions of the type of boiling-over eruptions with continuous pulses. During the eruptions, it is thought that the flooding of repeated ash flows almost not occurring ash cloud had created so voluminous ash-flow tuffs that were accumulated inside the caldera. However, the earlier eruptions also produced ash-flow tuffs rich in lithics, because the ash flows occurred along ring fracture forming a caldera. Because the thick ash-flow tuffs helped longer preservation of high temperature in the caldera, they resulted in dense welding as well as high devitrification.

4.3 Fallout tuffs

Fallout tuff consists of pyroclastic rocks and tuffites. If the lithofacies are classified based on grain size and sedimentary structures, the pyroclastic rocks correspond to the planar-bedded tuff, whereas the tuffites comprise planar-bedded tuffaceous sandstone and massive tuffaceous mudstone.

Planar-bedded tuff is pale bluish green or gray in color and consists of medium to fine-grained ashes and extends laterally without any variations in thickness (**Figure 5d**). The lithofacies, which are about 1 m in thickness, are intercalated between ash-flow tuffs in medial or distal parts of northern and eastern margins of the caldera (**Figure 4b**). The lithofacies have poor sorting and normal grading that is finely grained upward in a single bed and rarely include accretionary lapilli ranging 5~10 mm in size, so they are easily recognized as a fallout tuff. No cross bedding or erosion tracks are discovered. The lithofacies is a vitric tuff that is mostly composed of vitric shards and scarce crystal grains. Crystal fragments consist of plagioclase, and quartzes are less than 1 mm in size and angular in shape. Evidences that the lithofacies are medium to fine in grain size and thinly intercalated between ash-flow tuffs indicate that the fallout tuff was derived from ash cloud following the ash flows. The fallout phase, derived from ash cloud, lies over the ash-flow tuff. Thus, the fallout tuff appears as a top facies following the normal facies of ash-flow tuff. Additionally, the lithofacies occurring in either medial or distal parts of northern and eastern margins of caldera suggests that their crater was located in the southwestern part of the caldera. Because the fallout phase derived from ash cloud becomes abundant as it goes away from the crater, it is almost not observable in the proximal part near the crater but most dominant in the distal part.

5. Postcollapse intrusions

Postcollapse intrusions in the Guamsan caldera are composed of rhyolitic dikes (60.65 Ma in [9]) and plugs, which are exposed as several lithofacies which

are presumably connected to the identical magma chamber beneath the caldera. Based on differences in igneous structures and chemical composition, the lithofacies can be roughly subdivided into flow-banded rhyolite, porphyritic rhyolite, porphyritic rhyodacite, and stony rhyolite. In the field, a single rock body shows change in lithofacies within a few 100 m or a few km. In such cases, the erosion level in the Guamsan caldera area may nearly be approaching the original roof of the intrusions. Thus, according to positions related to the caldera-forming eruption, the intrusions can be categorized into intracaldera intrusions and ring dikes (**Figure 1**). The intrusions into the higher level of the Guamsan Tuff can demonstrate that they are the roots of postcollapse volcano, because the Guamsan Tuff has been of the final products and placed at a higher level as the caldera was formed [12].

5.1 Intracaldera intrusions

The intracaldera intrusions are intruding the Guamsan Tuff in the moat between the center and margin of caldera to form shapes of irregular circular plugs and straight dikes (**Figure 1**). In particular, they are annually distributed to form a circular ring shape along the caldera moat. Their exposure area is much wider in circular plugs than in straight dikes. The intrusions mostly consist of flow-banded rhyolite and rare spherulitic rhyolite in lithofacies. The rhyolite is mostly reddish gray in color and glassy and rarely contains plagioclase phenocrysts. Further, it develops flow foliations, especially spherulitic structure in the northern plug. The flow foliations have strikes almost parallel to intrusive contacts as well as steep dips ranging from 40 to 75°.

The lithofacies and occurrence patterns reflect that they are a vent region widened during the eruption of lava from residual magma rising through existing vents or fissures created due to crumpling by the collapse of the Guamsan caldera. In particular, the development of spherulitic structure in northern plugs is remarkable in contact with the fallout tuff. Therefore, the structure is to have been radially crystallized into vapor-phase crystallization by the moisture effect within the fallout tuff when the rhyolite intruded the tuff.

5.2 Ring dikes

Ring dikes occur along the caldera margin, and they can be categorized into the inner, intermediate, and outer ring dikes.

In terms of chemical composition, the dikes are mostly rhyolitic, whereas the southwestern ring dike is rhyodacitic in [2]. This indicates that the dikes are, chemically and mineralogically, similar to the Guamsan Tuff; this suggests that the ring dikes have a closely spatiotemporal relation with the caldera-forming eruption [13].

1. **Inner ring dike:** The dike is a combination of flow-banded rhyolite in the inner margin with stony rhyolite in the outer margin. The flow-banded rhyolite makes a steep slope in the inner margin of the ring dike. On the whole, the flow foliation is developed as closely spaced intervals and exhibits reddish gray to pale red colors. The flow-banded rhyolite is poor in phenocryst and alternates with very thin glassy bands and microcrystalline bands. The absence in phenocrysts seems to be the consequence of filter-pressing that passed only liquid except for crystals when magma was injected through fracture by compression in magma chamber. The glassy and microcrystalline textures indicate that the rhyolite was rapidly cooled because of the loss of volatile materials during magma rising instead of heat loss into conduit wall.

Stony rhyolite is frequently called felsite. It has a pale pink to pale gray color and indistinct or no flow foliation and rarely contains very tiny phenocrysts of quartz and feldspars. Under a microscope, quartz phenocrysts are rarely bipyramid in shape or embayed by resorption. The groundmass exhibits an intergranular texture by crystallization into microcrystalline to cryptocrystalline grain size. Therefore, according to the crystallinity, the earlier emplacement of inner side was followed by sequential intrusions after caldera collapse.

2. **Outer and intermediate dikes:** The outer ring dike intrudes along contact with the caldera and has contact with sedimentary rocks, Jugjang Volcanics, Naeyeonsan Tuff, and Muposan Tuff. The intermediate ring dike branches off inward from the southeastern part of the outer ring dike and then joins together at the south part; two small branches extend from the inner margin. The lithofacies exhibit whitish gray, pale gray, pale green, and pale pink colors, and they only show flow foliation in narrow dikes. They lack spherulite texture but represent stony or porphyritic textures. Thus, the outer ring dike shows stony rhyolite in the western and northern parts, porphyritic rhyolite in the eastern part, and porphyritic rhyodacite in the southern part, in which both are gradual. Further, the dike includes intrusive tuff in the northern part. In addition, the intermediate ring dike mostly consists of stony rhyolite.

Stony rhyolite contains microphenocrysts of plagioclase and alkali feldspars and accompanies tiny amounts of quartz and opaques. The phenocrysts are below 1 mm in diameter and are very small in content but also vary significantly depending on the locations. Occasionally, the rhyolite gradually converts into porphyritic rhyolite. The groundmass is mostly of quartzofeldspathic and occasionally contains biotite or opaques.

Porphyritic rhyolite contains phenocrysts of quartz, alkali feldspars, and plagioclase and rarely accompanies opaques. Quartz phenocrysts, up to 3 mm across, show embayed outline by significant resorption and contain rarely microcrystalline inclusions and occasionally bipyramid crystals. Some plagioclases constitute glomerophenocrysts. The groundmass shows an intergranular texture consisting of microcrystalline crystals. It is difficult to determine the boundary of such lithofacies because of the gradational change between porphyritic rhyodacite and stony rhyolite.

Porphyritic rhyodacite is dominant in plagioclase phenocryst and rarely accompanies alkali feldspars, hornblende, biotite, and opaques. Phenocrysts locally show very significant variations in content. The plagioclase phenocrysts are euhedral in shape and show a faint zonal structure. The groundmass consists of microcrystalline or cryptocrystalline feldspar, quartz, biotite, etc.

On the whole, the ring dikes show textural changes such as flow-banded, porphyritic, and stony structures in going toward the outer ring dike from the caldera center and also exhibit gradually compositional variation from rhyolite to rhyodacite in passing through southwest from the central part. Because all these constitute the ring dikes, this suggests that they intruded through ring faults or fractures resulting from caldera collapse.

It is thought that the emplacement timings may be locally different between rhyolites and various lithofacies. The textural changes from the caldera center to the outer ring dike suggest that the injection speed of magma was faster in the inner ring dike than in the outer ring dike, and the cooling rate was so slow that magma could crystallize to coarser grains owing to an intrusion of magma through wider passage in outer ring dike. Alternately, the changes between flow-banded textures and others may imply for temporal pulsational intrusions that the earlier injection of much hotter magma into the inner ring fault was followed by the injection of less hot magma into the outer ring fault, and changes between stony and porphyritic

textures may also imply the sequential continuous intrusions of magma. However, the textural changes southwestward from the northern part of the caldera suggest that the erosion degree increased while going further southwestward.

The gradual compositional changes from the northern to southwestern parts of the caldera suggest in the sequential successive intrusion of magma that more silicic top of magma chamber first injected into the ring fracture zone, and then less silicic part of magma remaining down there injected into the zone sequentially. Therefore, the relationship between the two intrusions was the relationship between liquid and liquid. That is, the textural changes imply that rhyolite magma injected in the ring fracture was successively intruded by rhyodacite magma. The rhyolite magma was more evolved, with residual melt remaining sufficiently in the top of the magma chamber below the caldera block. First, the rhyolite magma was tapped in order to rapidly excavate fusible melt from the magma chamber, and then, second, the rhyodacite magma down there was successively tapped from the chamber [2].

6. Discussion

Interpretations of many outcrops in the Guamsan caldera area can reconstruct eruption types, caldera collapse, and volcanic processes. Now, the author will discuss the eruption types according to the volcanic processes involved with the caldera collapse. The Guamsan caldera area represents that the volcanic processes occurred in the following order: (1) Pyroclastic flow-forming eruption from column collapse, (2) caldera forming and vent shifting, (3) boiling-over eruption and ash-flow phase, (4) postcollapse intracaldera rhyolite intrusions, (5) postcollapse ring rhyolite dike intrusions, and (6) successive rhyodacite intrusion.

6.1 Pyroclastic flow-forming eruption from column collapse

The internal stratigraphic sequence of Guamsan Tuff can be analyzed so as to infer eruptions and their sequences. For cases of caldera-forming eruptions, the ideal internal sequence would comprise the following: (1) Plinian fallout eruption, (2) pyroclastic flow-forming eruption, and (3) effusive eruption. The initial Plinian eruption would turn into pyroclastic flow-forming eruption from collapsing the eruption column overloaded by the decrease in gas content, widening of the vent radius, etc. Therefore, the transition from fallout eruption to pyroclastic flow-forming eruption would be caused by the rapidly increasing discharge rate [14–16] and accompany the ejection of large volume of lithic fragments commonly forming coarse lag breccia [10, 17–19]. The transition connotes an initiation of new vents related to the caldera collapse [20]. However, not all pyroclastic flow-forming eruptions necessarily have an initial Plinian eruption [21, 22]. This may suggest that the vent radius was widened almost simultaneously with the collapse of vent area.

In the Guamsan area, it initiated with the Pelean eruption forming block and ash flows without the Plinian eruption. Evidences supporting an eruption include the block and ash-flow breccia, which possibly correspond to the lowest part of the Guamsan Tuff. The breccia that belongs to the pyroclastic breccia got accumulated on the slope of crater by pyroclastic flow. The mechanism forming the pyroclastic flow is dominated by the collapse of lava dome or eruption column. The fact that the lithofacies mainly consist of rhyolite blocks suggests that the Pelean eruption may have occurred by the temporary collapse of active lava dome, from which lava fragments flowed on a cone slope as block and ash flows. In addition, it turned into the eruptions forming strongly fluidized pyroclastic flow due to widening vent by collapse of the vent area. The eruption was probably a single vent phase erupted from a vent.

The lower member of Guamsan Tuff, overlying this breccia, consists of disorganized massive breccia, graded bedding tuff, lapilli tuff, block tuff, and sheet bedding tuff in lithofacies; the first three lithofacies correspond to pyroclastic flow rocks, while the last one belongs to fallout tuff. Because the fallout tuff mostly consists of ashes less than 1 mm in diameter, is less than 1 m thick, and is overlying each ash-flow tuff unit, it corresponds to the ash cloud-derived fallout phase rather than the Plinian fall phase. Thus, a pair of ash-flow tuff and fallout tuff represents the sedimentary phases of a flow unit and an ash cloud fallout unit that follow a pyroclastic flow. According to Sparks et al. [23], the flow unit corresponds to a main body of pyroclastic flow called layer 2, whereas the ash cloud fallout unit refers to layer 3. Here, the ground surge unit, called layer 1, is not recognized at the base. The ash-flow tuff without fallout tuff might be attributable to the successive pyroclastic flow that did not leave sufficient time to deposit fallout ash from ash cloud or to the rapid denudation of ash cloud-fallout deposits by fast violent pyroclastic flow near the crater. However, the pyroclastic flow-forming eruption successively occurred after the temporary Pelean eruption. Here, the mechanism forming pyroclastic flow was created by the collapse of the eruption column (**Figure 6a**).

The flow mechanism of pyroclastic flow represents partially fluidized flow [24–26]; the mechanism of transportation and sedimentation is similar to that of debris flow with slight differences. That is, while big clasts are transported by fine-grained matrix and water in the debris flow, big lithic fragments are transported by fine ashes and gas in the pyroclastic flow. Most pyroclastic flows are laminar flows in their body, although they are turbulent flows in their head. Pyroclastic flow can be distinguished into the three types of non-expanded flow, expanded flow, and segregating flow based on fluidization behaviors [11]. The ash-flow tuffs, occurring in the lower tuff member of Guamsan Tuff, seem to have been mostly emplaced by the expanded flow. The normal grading of lithic fragments and inverse grading of pumices in the lower ash-flow tuffs are dominated by settling velocity that depends on their density difference from matrix. The lithic fragments will occur normal grading according to each settling velocity because of the higher density of lithic fragments than matrix, whereas the pumices will occur the inverse grading according to floating over because of the lower density than matrix. Such grading appears more distinctly in accordance with the increase in density difference from matrix, when becoming greater in expansion degree of pyroclastic flow. The flow process of gas included during fluidization causes grading and sorting of fine-grained ashes. According to the expansion degree, the highly expanded flow would detach a large volume of fine-grained ashes from the flow to ash cloud, whereas the less expanded flow would drift upward only a small volume. Because the ash-flow tuffs in the lower tuff member mostly belong to the category of expanded flow, they represent not only the normal grading of lithic fragments but also planar-bedded tuffs by falling from the ash clouds detached from pyroclastic flows.

6.2 Forming caldera and vent transmitting

The ash-flow tuffs and fallout tuffs in the lower member were supplied from the central vent (**Figure 6a**). With the gradually increasing discharge volume of magma, the top of the magma chamber began sinking down like a ring shape. Here, the collapse occurred off northeastward from the central vent. The pressure in the magma chamber decreased gradually as the tapping of magma continued, and then the collapse seemed to occur, when the underpressure in the magma chamber exceeded the strength of overlying rocks. The roof collapse may recover lithostatic pressure at the top of the magma chamber. In this way, the role of central vent was rapidly reduced simultaneously with the initial collapse of caldera. The following

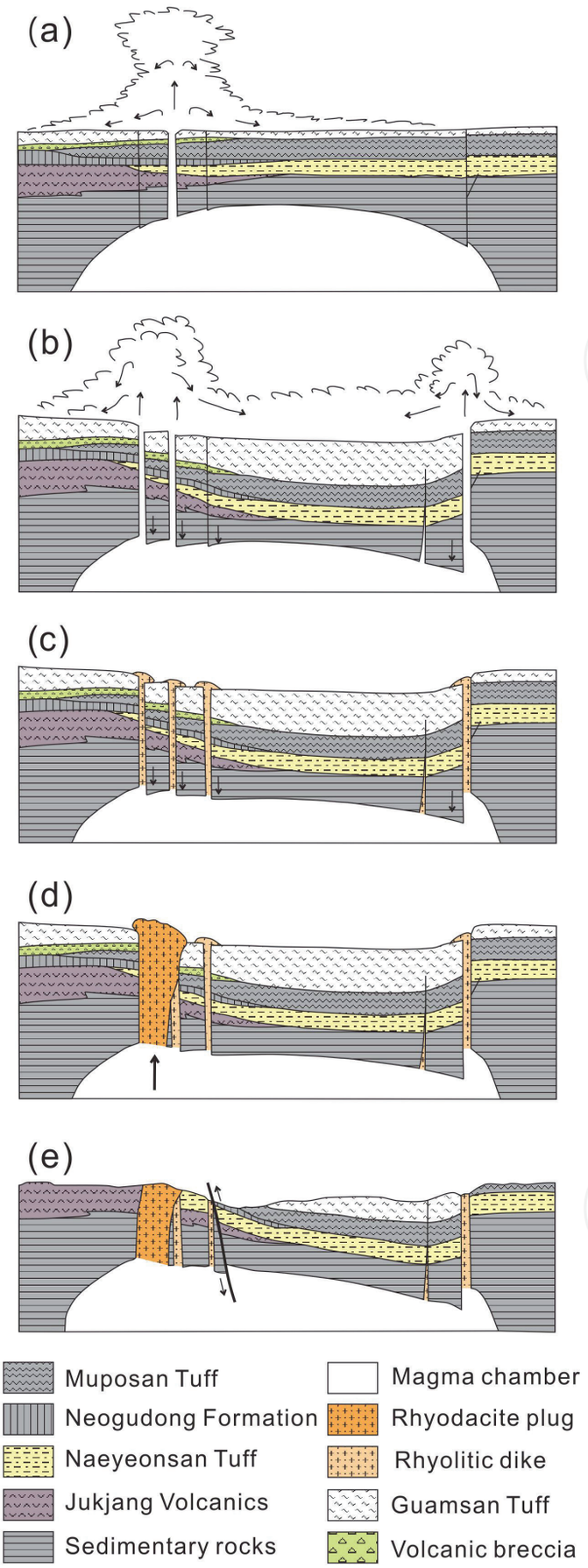

Figure 6.
Schematic sections, pictorially explaining the eruption types and volcanic processes in the Guamsan caldera. (a) Pyroclastic flow-forming eruptions through a central vent; (b) caldera collapse along ring fractures and boiling-over eruptions through multiple ring fissure vents; (c) effusive eruptions of rhyolitic magma through multiple vents along the intracaldera and ring fractures; (d) renewed rhyodacitic volcanism along the southwestern ring fracture; (e) present erosion surface.

ash flows were produced by erupting from many vents along the ring fracture zones, and then the caldera was collapsed further (**Figure 6b**). The pyroclastic flow-forming eruption with two-staged caldera-forming processes was already proposed by Druitt and Sparks [20].

The intercalation and lateral change of breccias in the Guamsan Tuff demonstrate that the collapse of Guamsan caldera is related with pyroclastic flow-forming eruption. This is directly evident in that the chaotic massive breccia is intruded as a wedge shape at the base of upper member of Guamsan Tuff. The breccia is a caldera-forming breccia produced by debris flow moving on steep caldera wall following the caldera collapse; this suggests the vent shift that connotes the fissure eruption. Thus, the appearance of breccia not only indicates the beginning with caldera collapse but also implies the closing of a single central vent as well as the initiation of multiple ring fissure vents. In addition, the Guamsan Tuff is nonexistent in extracaldera, whereas it is still over 850 m in thickness in intracaldera. Such thickness of the intracaldera tuffs is roughly three times thicker than the thickness of tuffs from extracaldera outflow, which is similar to cases of other tuffs from elsewhere around the world [12]. That is, this supports the fast accumulation of ash-flow tuff inside the caldera due to continuous eruption during the caldera collapse as opposed to collapsing the caldera after termination of the pyroclastic flow-forming eruption. Partial existence of intrusive tuff in northern ring dike can be counted as further evidence as well. In addition, although the lower member of Guamsan Tuff inside the caldera hardly exhibits welded zone but represents vitroclastic fabric, the upper member of Guamsan Tuff that exhibits welded foliation is dominant in eutaxitic and parataxitic fabrics and undergoing the devitrification process, leaving coarse-grained crystals. This is seemingly attributable to the high temperature that lasted for a long time by rapid accumulation of ash-flow tuff inside the caldera.

Thus, it is thought that the development of multiple ring fractures by caldera collapse during pyroclastic flow-forming eruption from central vent could serve as a natural momentum shifting to multiple vents along the ring fractures concurrently with the closing of a single vent.

6.3 Boiling-over eruption and ash-flow eruption

Some volcanologists have suggested from the two-staged models that the pyroclastic flow-forming eruptions converted into ring fracture vents from a single vent related with a caldera [17, 18], occasionally into the eruption from ring fractures [18, 27]. It seems to be the direct main cause that the shifting vents into ring fractures were transformed into the boiling-over eruption from the pyroclastic flow-forming eruption by column collapse. The conversion into boiling-over eruption was attributable to the rapidly increasing discharge of magma; the increase in discharge was possible from sinking the caldera block into magma chamber along the outward dipping of ring fracture zones. That is, because of the increasing number of vents together with outward dipping of ring fracture zones, the conduits were naturally gradually widened, and instantaneous discharge rate was rapidly increased as the subsidence occurred. Accordingly, the eruption at this moment did not form high eruption column but turned into the boiling-over eruption that produced a large volume of ash flow (**Figure 6b**). The discharge rate of magma at this moment was much higher than the discharge rate necessary for maintaining the eruption column.

In addition, the naturally widening conduits along subsidence were not necessary for eroding the conduit walls. Accordingly, the lithic fragments rapidly decrease in volume and are much smaller in size within the upper ash-flow tuffs as

compared to the lower ash-flow tuff. It is very difficult to distinguish boundaries between each flow unit because of the fewer lithic fragments in the upper ash-flow tuffs, which are densely welded or even almost completely liquefied and devitrified enough to form eutaxitic and parataxitic fabrics. If it would form highly welded tuffs, it should be slow and less fluidized non-expansive ash flows, and it should be thickly accumulated during a short period, by the low column collapse derived from high-temperature magma, because heat loss could be prevented through the production and flooding of high-temperature ash flows. In order to reduce the height of the eruption column in this way, it is possible for magma to have a higher discharge rate, lower gas diffusion rate, and less gas content during eruption. Under such conditions, the ash flows may not spread far away and diminish with the loss of vitric ashes. Such pyroclastic flow-forming eruptions also indicate that they originated from nonviolent voluminous eruption, which supports that they were boiling-over eruptions that successively occurred without near explosiveness. The eruptions could produce voluminous ash-flow tuffs by flooding repetitive ash flows that do not almost produce ash cloud, whereas they did not have chances to accumulate fallout tuff.

The ring fissure eruption which caused such phenomena converted into effusive eruption together with the injections of magma into fissures by exhausting its explosive force and continuously collapsing caldera block due to the rapidly increasing eruption volume.

6.4 Intrusion of postcollapse intracaldera rhyolites

The boiling-over eruptions through ring fractures were also converted into non-explosive activities of magma by an exhaustion of volatile materials due to eruptions of voluminous ash flows. With the caldera formation, the residual magma were intruded into fissures of inverse wedge-like shape formed in the existing vent or in moat, and effusive eruptions successively occurred through the fissures (**Figure 6c**). The evidence for this is that the rhyolites occur in the moat as modes of a plug or dikes.

This also suggests that the distribution pattern of these rhyolites is dominant in fissures made in the moat along the caldera collapse. Thus, it is thought that the rhyolites are products of residual magma that filled fissures in the moat by the pressure imposed to the magma chamber after caldera collapse. Though volcanic domes formed at this time had already disappeared by erosion and denudation, it is presumable that they may have connected to the magma chamber as roots of postcollapse volcano with dome shape.

The following points of evidence suggest that they are intrusive roots of volcanoes after the collapse of caldera. Flow foliations in the rhyolite plugs dip almost vertically inside the caldera, whereas they dip toward the center outside the caldera. The intrusion of these rhyolites up to the high level of the Guamsan Tuff through fissures in the moat suggests that these are the roots of volcanoes after the collapse of caldera occurred at the higher level. The contacts of the rhyolites with Guamsan Tuff without cooling margin and the chemical composition of rhyolites similar to Guamsan Tuff also indicate that the intrusion of rhyolites was that the volcanic event occurred directly following the eruption of ash flows. That is, the intrusions can be regarded as underground residuals of volcanic activity occurring along the intracaldera fissures. At that time, the residual magma was probably very viscous and could not flow far away, fill only fissures up or at the upmost, and form small domes on the surface. Because they contain almost no phenocryst and develop flow foliation, they would perhaps have formed small lava domes on the ground.

6.5 Intrusion of postcollapse ring rhyolite dikes

Following the formation of the Guamsan caldera together with the ash flow-forming eruptions along the ring fracture, the residual magma formed ring rhyolite dikes by gradual injection into ring faults (**Figure 6c**). The injection of magma into ring fault, which is driven by the overpressure of magma causing its buoyance, can form dikes without any erosion of wall rocks [28]. The dikes are considered to be intrusion roots of several volcanoes created along the ring fracture after the caldera collapse. It is supposed that the volcanoes would have formed rhyolite domes aligned along the ring fracture on the ground. This is because the flow foliations in the ring dikes dip sub-vertically inside the caldera, whereas they dip inward outside the caldera.

At the same time as the intrusion of intracaldera rhyolites, the residual magma began with rising into ring fracture zones by the force accumulated therein. At that time, the residual magma was injected mainly into ring fissure vents, which were the passage of later ash-flow tuffs, and then formed the ring rhyolite dikes (**Figure 6c**). These are also a series of small postcollapse volcanoes that formed several rhyolite domes.

The rhyolites in ring dikes are generally glassy or microcrystalline in terms of crystallinity without cooling margins and distinct dragging in contact with adjacent rock body, implying that the dikes intruded the fissures along the ring fracture zones. That is, the ring dikes indicate that it is closely involved in the collapse of Guamsan caldera. Comparing the fact that the inner dikes are dominantly glassy with flow-banded to stony feature, the outer dikes are dominantly with stony to porphyritic texture and no cooling margins at the contact; this should be explained as a consequence of temporary pulsational intrusions, considering that magma chamber may be cooled down inward from the outside. However, sequential successive intrusion should be explained simultaneously, because the lithological relations in the outer and intermediate ring dikes are gradational. Such a relationship is strongly supported by the gradual compositional changes explained in the following.

6.6 Successive intrusion of rhyodacite

Following the intrusion of ring rhyolite dikes, the sequential successive intrusions of rhyodacite occurred in the junction site of outer and intermediate ring dikes in southwest part of the caldera (**Figure 6d**). The reason for this is that both dikes have the gradational lithology in the contact. Besides, the rhyodacites perhaps were intruded from the more crystallized inner part of the magma chamber which was cooled down inwardly from its margin and top. This is because, as compared to the rhyolite dike, which is mostly glassy to microcrystalline, the rhyodacite at the junction part exhibits a coarser texture that is porphyritic and microcrystalline.

The gradual change from rhyolite to rhyodacite in the outer ring dike suggests that the more silicic top of magma chamber was earlier injected along the ring fracture zone and following on it the more mafic magma below it was successively intruded. The emplacement of rhyodacite in the ring dike was possible by discharging the rhyodacite magma following after exhaustion of effective melt by tapping the rhyolite magma [2]. By accounting for the patterns and locations of the ring dikes, the dikes can be judged to be the products of magma rising along the junction part of two ring fracture zones during the final stage of Guamsan volcanic activities; thus, they are also regarded as the roots of postcollapse volcanoes connected to the magma chamber.

The intrusion of this rhyodacite resulted in slow crystallization after rising magma emplaced through the junction part of ring dikes; this implies the closure of the Guamsan volcanic activities. Therefore, this spatiotemporal view corresponds to

a final intrusion along the ring fracture zone of southwestern caldera in Guamsan magmatic system, but they now display their root zones due to deep erosions during long time (**Figure 6e**).

7. Conclusions

Stratigraphic units associated with the Guamsan caldera comprise Guamsan Tuff and rhyolitic intrusions. Guamsan Tuff typically consists of volcanic breccia, ash-flow tuffs, and fallout tuffs, of which the ash-flow tuff is very dominant.

Volcanic breccia can be distinguished into the block and ash-flow breccia at the lower part and the caldera-collapse breccia at the upper part, according to their distribution locations and stratigraphic sequence. In the lower member, the ash-flow tuffs exhibit expansive pyroclastic flow phase by the pyroclastic flow-forming eruptions, and the fallout tuffs exhibit ash cloud-falling phase, whereas the ash-flow tuffs in the upper member exhibit the non-expansive ash-flow phase by the boiling-over eruptions.

Rhyolite intrusions can be distinguished into intracaldera intrusions and ring dike based on location and pattern: the ring dikes are distinguished into the inner, intermediate, and outer ring dikes. The Guamsan caldera represents a caldera cycle connecting into ash-flow tuff—caldera—ring dikes.

The volcanic processes in the Guamsan caldera area can be summarized as the following sequence along the caldera cycle: (1) The volcanic activity began with the Pelean eruption generating block ash-flow phase by a lava dome, and (2) it then subsequently turned into the fluidized pyroclastic flow phase by the collapse of high eruption column. At that time, fluidization of the pyroclastic flow was reduced with gradual decrease in the height of the eruption column. (3) In the transformation into ash-flow phase, boiling-over eruptions burst instantaneously hotter pyroclastic materials to be densely welded. The boiling-over eruptions began on their way by migrating vents into ring fracture zones together with the caldera collapse. At the earlier stage of eruption, the pyroclastic flows were produced from a central vent, whereas voluminous ash flows were generated from multiple vents in the ring fracture zone. The consequently accumulated Guamsan Tuff was at least 850 m thick inside the caldera. (4) After the ash-flow eruptions, the magma was injected into fissures in the caldera moat to form the rhyolitic plug and dikes. (5) Almost simultaneously, the magma was successively injected along the ring fracture zone so as to form the ring rhyolite dikes. (6) Finally, the rhyodacite was successively intruded into the junction part of southwestern ring dikes.

Acknowledgements

The work was supported by funding of the Korea Meteorological Administration Research and Development Program under Grant KMI (**2018-01610**) through the Korea Meteorological Institute. We are grateful for the careful approval for our proposal by the editor and reviewer, Professor Angelo Paone.

Author details

Sang Koo Hwang
Department of Earth and Environmental Sciences, Andong National University, Andong, Korea

*Address all correspondence to: hwangsk@anu.ac.kr

References

[1] Hwang SK. Collapse type and evolution of the Guamsan caldera, southeastern Cheongsong, Korea. Journal of the Geological Society of Korea. 2002;**38**:199-216

[2] Hwang SK. Magmatic evolution of volcanic rocks related with the Guamsan caldera, southeastern Korea. Journal of the Geological Society of Korea. 2002b;**38**:293-310

[3] Lee SM, Kim SW, Jin MS. Cretaceous to tertiary volcanic activities and tectonic significance of South Korea. Journal of the Geological Society of Korea. 1987;**23**:338-359

[4] Hwang SK, Kim SW. Petrology of cretaceous volcanic rocks in the Milyang-Yangsan area: Petrotectonic setting. Journal of the Geological Society of Korea. 1994;**30**:229-241

[5] Chough SK, Kwon S-T, Ree J-H, Choi DK. Tectonic and sedimentary evolution of the Korean peninsula: A review and new view. Earth-Science Reviews. 2000;**52**:175-235

[6] Hwang SK. Tectonic setting and arc volcanisms of the Gyeongsang arc in the southeastern Korean peninsula. The Journal of the Petrological Society of Korea. 2012;**21**:367-383

[7] Hwang SK. SHRIMP U-Pb dating and volcanic history of the Jipum Volcanics, western Yeongdeok, Korea. The Journal of the Petrological Society of Korea. 2017;**26**:341-352

[8] Hwang SK, Jo IH, Yi K. SHRIMP U-Pb zircon dating and stratigraphic relationship of the Bunam stock and Muposan tuff, Cheongsong. Journal of the Geological Society of Korea. 2016;**52**:405-419

[9] Hwang SK, Jo IH, Yi K. SHRIMP U-Pb dating and volcanic processes of the volcanic rocks in the Guamsan caldera, Korea. Economic and Environmental Geology. 2017;**50**:467-476

[10] Wright JA, Walker GPL. The ignimbrite source problem: Significance of a co-ignimbrite lag-fall deposits. Geology. 1977;**5**:729-732

[11] Wilson CJN. The role of fluidisation in the emplacement of pyroclastic flows: An experimental approach. Journal of Volcanology and Geothermal Research. 1980;**8**:231-249

[12] Lipman PW. Roots of ash-flow calderas in western North America: Windows into the tops of granitic batholiths. Journal of Geophysical Research. 1984;**89**:8801-8841

[13] Smith RL, Bailey RA. Resurgent cauldrons. Geological Society of America, Memoir. 1968;**116**:613-662

[14] Bursik MI, Woods AW. The dynamics and thermodynamics of large ash flows. Bulletin of Volcanology. 1996;**58**:175-193

[15] Hwang SK, Lee GD, Kim SW, Lee YJ. Volcanisms and volcanic processes of the Wondong caldera, Korea. The Journal of the Petrological Society of Korea. 1997;**6**:96-110

[16] Hwang SK, Kim SW, Lee YJ. Volcanisms and igneous processes of the Samrangjin caldera, Korea. The Journal of the Petrological Society of Korea. 1997;**7**:147-140

[17] Druitt TH. Vent evolution and lag breccia formation during the Cape Riva eruption of Santorini, Greece. Journal of Geology. 1985;**93**:439-454

[18] Druitt TH, Bacon CR. Lithic breccia and ignimbrite erupted during the collapse of Crater Lake caldera, Oregon.

Journal of Volcanology and Geothermal Research. 1986;**29**:1-32

[19] Rosi M, Vezzoli L, Aleotti P, De Censi M. Interaction between caldera collapse and eruptive dynamics during Campanian ignimbrite eruption, Phlegrean fields, Italy. Bulletin of Volcanology. 1996;**57**:541-554

[20] Druitt TH, Sparks RSJ. On the formation of calderas during ignimbrite eruptions. Nature. 1985;**310**:679-681

[21] Francis PW, O'Callaghan L, Kretzchmar GA, Thorpe RS, Sparks RSJ, Page RN, et al. The Cerro Galan ignimbrite. Nature. 1983;**301**:51-53

[22] Hwang SK, Kim SW. Silicic volcanism of Yangsan caldera, Korea. Journal of the Geological Society of Korea. 1992;**28**:491-503

[23] Sparks RSJ, Self S, Walker GPL. Products of ignimbrite eruptions. Geology. 1973;**1**:115-118

[24] Sparks RSJ. Grain size variations in ignimbrites and implications for the transport of pyroclastic flows. Sedimentology. 1976;**23**:147-188

[25] Sparks RSJ, Bursik MI, Carey SN, Gilbert JS, Glaze LS, Sigurdsson H, et al. Volcanic Plumes. Chichester: Wiley; 1997. p. 574

[26] Branney MJ, Kokelaar P. Pyroclastic density currents and sedimentation of ignimbrites. Geological Society, London, Memoirs. 2002;**27**:143

[27] Hildreth W, Mahood GA. Ring-fracture eruption of the bishop tuff. Geological Society of America Bulletin. 1986;**97**:396-403

[28] Gudmundsson A, Marinoni LB, Marti J. Injection and arrest of dykes: Implications for volcanic hazards. Journal of Volcanology and Geothermal Research. 1999;**88**:1-13